

## Vibration Characteristics of Aircraft Engine-Bladed-Disk Assembly

J. S. RAO, C. B. SHAH & CH. L. GANESH

Indian Institute of Technology, New Delhi-110016

Y. V. K. S. RAO

Vikram Sarabhai Space Centre, Trivandrum-695022

Received 25 April 1984

**Abstract.** This paper is concerned with the vibration characteristics of a gas-turbine blade-disk assembly and a third stage of compressor blade-disk assembly of an Orpheus aircraft engine. The assembly is analyzed by considering each component individually and then combining them together with a **receptance** coupling technique by matching forces and displacements at each junction point. The blade is **modelled** by number of free-free aerofoil section beams staggered at different angles to the plane of the disk, and the non-uniform disk is **modelled** as **number** of concentric **annuli**. The natural frequencies and mode shapes for each case have been obtained. Results obtained are verified by testing both the above assemblies on a micro-processor based vibration exciter and real time analyzer. The mode shape corresponding to each natural frequency was obtained by probing with hand held accelerometer.

### Nomenclature

- $A$  Area of cross-section of blade
- $A$ , Coefficient matrix at radius  $r$
- $\dot{b}$   $K.r$
- $D$   $2Eh^3/(3(1 - \nu^2))$
- $E$  Modulus of elasticity
- $G$  Modulus of rigidity
- $h$  Half thickness of disk

$I$  Moment of inertia of blade

$I_n(K.r), J_n(K.r), K_n(K.r), Y_n(K.r)$  Bessel functions of order  $n$

$I'_n(K.r), J'_n(K.r), K'_n(K.r), Y'_n(K.r)$  Derivatives of Bessel functions  
w.r.t. the argument

$J$  Constant ( $GJ =$  Torsional rigidity)

$j$  Number of disk **annulus**

$K^4$   $2\omega^2 \cdot \rho \cdot h/D$

$L$  Length of the blade

$I$  Variable for the blade length

$M$  Bending moment

$M_d$  Mass of the disk

$M_p$  Polar moment of inertia

$N$  Number of blades

$n$  Nodal diameters

$Q$  Vector of internal loads

$4$  Vector of displacements

$r^{\wedge}$  Radius of disk

$S$  Shear force

$u_1$   $n^2 (1 - \nu)$

$u_2$   $-b (1 - \nu)$

$u_3$   $u_1 + b^2$

$u_4$   $u_1 - b^2$

$V(r)$  State vector expressions,  $(q, \partial q_1/\partial r, S, M)$

$\alpha$  (n) Disk receptance for  $n$  nodal diameter

$\beta$  Blade receptance

$\beta', \beta'', \beta'''$  Blade root, blade root-tip and blade tip receptances

$[\beta_1], [\beta_2], [\beta_3]$  Receptance matrices of blade elements 1, 2 and 3

$[\beta_{12}]$  Coupled receptance matrix of blade elements 1 and 2

$[\beta_{123}]$  Coupled receptance matrix of blade elements 1, 2 and 3

$\Delta$  System receptance (or frequency) matrix

- $\theta$  Angular coordinate
- $\lambda^4$   $\omega^2 \cdot \rho \cdot A / EI$
- $\rho$  Mass density
- $\omega$  frequency
- $\nu$  Poisson's ratio

**Subscripts**

- B** Blade root
- D** Disk rim
- i** Inner edge of **annulus**
- o** Outer edge of **annulus**
- p** Polar moment
- 1** Axial translation (disk)
- 2** Tangential rotation (disk)
- 3** Tangential translation (disk).
- 4** Axial rotation (disk)
- 5** Radial rotation (disk)
- 6** Radial translation (disk)

**1. Introduction**

In aircraft gas-turbines, **catastrophic** failures have occurred when turbine assemblies have failed owing to large amplitude of vibration. To avert such failures it is essential to accurately predict the natural frequencies and mode shapes of the assembly, in order to avoid strong resonances with anticipated excitation frequencies in the operating speed range of the rotor.

The importance of analyzing the complete blade-disk assembly in order to **study** turbine blade vibration is now well established. The main reason being that interblade coupling through the disk contributes significantly to the nature of the basic vibration properties. In actual engine assembly, the frequencies in lower modes are influenced by the thickness of the disk hub and the radius of attachment, while the higher order modes are more influenced by rim thickness and the geometry of blade attachment. Thus, for a realistic situation, it is important to consider the non-uniformity in thickness of disk (hub, disk rim), the blading and also the twist of the blade. The data obtained experimentally for natural frequencies and mode shapes and also for resonant vibration response levels, can only be fully understood by referring to such an analysis.

**Armstrong**<sup>1,2</sup>, is one of the earliest workers to use receptance coupling **technique**<sup>3</sup>— to couple the disk and blade motions; he assumed that all blades are identical, there by applying the receptance coupling procedure to just two components only; the disk and the blading. He also presumed the form of modes of vibration and his analysis is restricted to system with large number of blades and also carried out extensive **tests** on assembly comprising of uniform disk and uniform rectangular blades staggered at specified angle. **Ewins**<sup>4</sup> eliminated the limitations inherent in Armstrong's analysis. He considered a disk to be bladed with a set of non-identical blades and no assumptions of model shape nor restriction to the number of blades required, were made. **He**<sup>5</sup> later studied the effects of bladed disk and also studied the dynamic characteristics of a system having pairs of close natural frequency modes, when it is forced to vibrate under typical operating conditions with-excitation being derived from the presence of obstruction in flow. **He**<sup>6</sup> later summerized all his previous works and presented an analysis to predict the fundamental vibration characteristics of a complete bladed-disk assembly. He also concluded that a detuned system is susceptible to many more resonances than is an equivalent tuned system. The effects of adding various types of shrouds, have been studied by Cottney'. Cottney & **Ewins**<sup>8</sup> made an investigation aimed at improving the efficiency of shrouded bladed-disk assemblies. The assembly is analyzed by studying each component individually and then combining them together with receptance coupling procedure by matching forces and displacements at each connecting point.

The analysis of Cottney & **Ewins**<sup>7,8</sup> has been adopted here to develop computer program, in order to find natural frequencies and corresponding mode shapes for the turbine and the compressor stage assemblies. In this analysis we considered the system as having just two components- the disk and blading which are interconnected at the junction, i.e., disk-rim/blade-root. The blade elements **are** treated as aerofoils instead of rectangular cross-section beams. Six degrees of freedom-three translational and three rotational directions, are used at each blade-disk junction. A computer program is developed to determine the natural frequencies and mode shapes. Tests on the **gas**-turbine stage and the third stage of the compressor of an Orpheus aircraft engine are carried out to validate these programs. Good agreement between the analytical and experimental **results** has been obtained.

## 2. Theory

### 2.1 Receptances of a Multi-Stage Disk

From equilibrium considerations of a plate, expressions relating the **flexural** deformations to three types of internal loads, viz., shear force, bending moment and twisting moment can be obtained. These loads will be in equilibrium with an externally applied axial force, a tangential torque and radial torque respectively at the rim. The shear deformation within the plate is ignored in the following :

Consider a disk composed of  $j$  annuli, excited at the rim by forces as shown in Fig. 1. In order to satisfy the compatibility and equilibrium across the internal boundary separating any two annuli, it is sufficient to ensure that

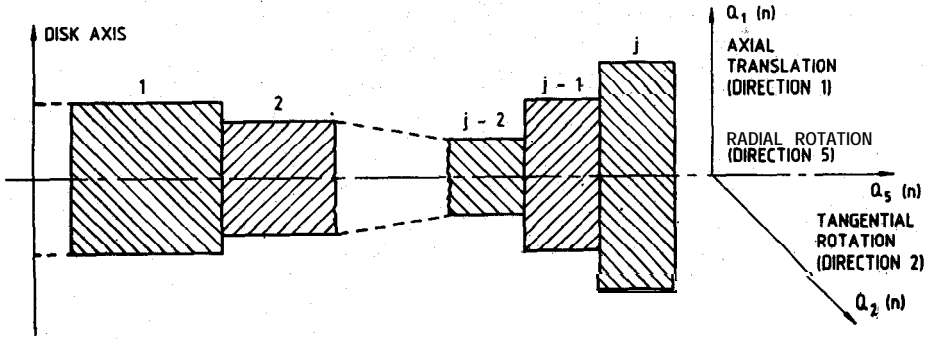


Figure 1. Configuration of disk annuli and coordinates used for analysis of bladed disk.

$$\left. \begin{aligned} (q_1)_j &= (q_1)_{j-1} & ; & \left( \frac{\partial q_1}{\partial r} \right)_j = \left( \frac{\partial q_1}{\partial r} \right)_{j-1} \\ \left( \frac{\partial^2 q_1}{\partial r^2} \right)_j &= \left( \frac{\partial^2 q_1}{\partial r^2} \right)_{j-1} & ; & \left( \frac{\partial^3 q_1}{\partial r^3} \right)_j = \left( \frac{\partial^3 q_1}{\partial r^3} \right)_{j-1} \end{aligned} \right\} \quad (1)$$

Let  $V(r)$  be a vector defined by

$$\{V(r, j, n)\} = \begin{Bmatrix} q_1 \\ \frac{\partial q_1}{\partial r} \\ S(r) \\ M(r) \end{Bmatrix} \quad (2)$$

at the inner edge of  $j$ th annulus. In the above

$$S(r) = Q_1(n) - \frac{1}{r} \frac{\partial Q_5(n)}{\partial \theta} \quad (3)$$

and

$$M(r) = - Q_2(n) \quad (4)$$

where  $n$  denotes nodal diameter.

Let  $X_j$  be the vector of integration constants for  $j$ th annulus which is determined by boundary conditions and let  $[A(r)]$  be a matrix of coefficients for  $j$ th the annulus, such that

$$\{V(r)\} = [A(r)]_j \{X\}_j$$

$$\{V(r_{j,0})\} = [A_l]_j \{X\}_j$$

(5)

and

$$\{V(r_{j,0})\} = [A_0]_j \{X\}_j$$

The  $[A(r)]$  matrix can be written as, (reference 9)

$$[A(r)] = \begin{pmatrix} J_n & Y_n & I_n & K_n \\ K.J'_n & K.Y'_n & K.I'_n & K.K'_n \\ \frac{D}{r^2}(J'_n b u_3 - J_3 u_1) & \frac{D}{r^2}(Y'_n b u_3 - Y_n u_1) & \frac{D}{r^2}(I'_n b u_1 - I_n u_1) & \frac{D}{r^2}(K'_n b u_3 - K_n u_1) \\ \frac{D}{r}(J_n u_4 + J'_n u_2) & \frac{D}{r}(Y_n u_4 + Y'_n u_2) & \frac{D}{r}(I_n u_3 + I'_n u_2) & \frac{D}{r}(K_n u_3 + K'_n u_2) \end{pmatrix} \quad (6)$$

where

$$u_1 = h^2 (1 - \nu), u_2 = -b (1 - \nu), u_3 = u_1 + b^2, u_4 = u_1 - b^2 \quad (7)$$

As there are no loads at the inner edge of the innermost annulus, we get

$$\begin{Bmatrix} 0 \\ 0 \end{Bmatrix} = \begin{bmatrix} 0 & 0 & 1 & 0 \\ 0 & 0 & 0 & 1 \end{bmatrix} [A_l]_1 \{X\}_1 \quad (8)$$

For compatibility and equilibrium between the adjacent edges of the (j-1)th annulus & jth annulus, using Eqns. (I), (5) and (8) for the boundary conditions at the innermost edge, we get

$$[B] \{X\}_j = \begin{Bmatrix} 0 \\ 0 \\ S(r_{j,0}) \\ M(r_{j,0}) \end{Bmatrix} \quad (9)$$

where

$$[B] = \begin{pmatrix} \begin{bmatrix} 0 & 0 & 1 & 0 \\ 0 & 0 & 0 & 1 \end{bmatrix} [A_l]_1 & [A_0]_1^{-1} & [A_l]_2 & \cdots & [A_l]_j \end{pmatrix} \quad (10)$$

Now, to find disk receptances,  $u(n)$ , let the state vector at the disk rim,  $(r_{j,0}) = r_D$ , be given as

$$\{V(r_{j,0})\} = [A_0]\{X\}_j = [A_0][B]^{-1} \begin{Bmatrix} 0 \\ 0 \\ S(r_{j,0}) \\ M(r_{j,0}) \end{Bmatrix} \quad (11)$$

If a unit axial force,  $Q_1(n)$ , alone is applied to the rim then

$$\begin{Bmatrix} q_1(n) \\ \frac{\partial}{\partial r} q_1(n) \end{Bmatrix} = \begin{bmatrix} 1 & 0 & 0 & 0 \\ 0 & 1 & 0 & 0 \end{bmatrix} [A_0]_j [B]^{-1} \begin{Bmatrix} 0 \\ 0 \\ 1 \\ 0 \end{Bmatrix} \quad (12)$$

Alternatively, if a unit tangential torque alone is applied, then the bending moment  $M(r_{j,0})$  will be unity, and the receptance matrix for directions 1 and 2 may be written as

$$\begin{bmatrix} \alpha_{11}(n) & \alpha_{12}(n) \\ \alpha_{21}(n) & \alpha_{22}(n) \end{bmatrix} = \begin{bmatrix} 1 & 0 & 0 & 0 \\ 0 & -1 & 0 & 0 \end{bmatrix} [A_0]_j [B]^{-1} \begin{bmatrix} 0 & 0 \\ 0 & 0 \\ 1 & 0 \\ 0 & -1 \end{bmatrix} \quad (13)$$

The receptances due to a rim radial torque may be evaluated as

$$\begin{aligned} \alpha_{15}(n) &= \frac{n}{r_D} \alpha_{11}(n) \\ \alpha_{25}(n) &= \frac{n}{r_D} \alpha_{21}(n) \end{aligned} \quad (14)$$

and

$$\alpha_{55}(n) = \left(\frac{n}{r_D}\right)^2 \alpha_{11}(n)$$

The receptance matrix  $[a(n)]$  is symmetric. The remaining receptances relate to the in-plane motion of the disk and may be assumed zero except for the 1 and 0 nodal diameter modes. In these modes rigid body displacements are possible. For 1 diameter mode,

$$\mathbf{a} \quad [\alpha(1)] = \begin{bmatrix} \alpha_{11}(1) & \alpha_{12}(1) & 0 & 0 & \frac{1}{r_D}(1) & 0 \\ & \alpha_{22}(1) & 0 & 0 & \frac{\alpha_{12}(1)}{r_D} & 0 \\ & & I & R_1 & 0 & -R_1 \\ & & & & 0 & 0 \\ \text{Symmetric} & & & & & 0 \\ & & & & & R_1 \end{bmatrix} \quad (15)$$

For 0 nodal diameter mode

$$[\alpha(0)] = \begin{bmatrix} \alpha_{11}(0) & \alpha_{12}(0) & 0 & 0 & 0 & 0 \\ & \alpha_{22}(0) & 0 & 0 & 0 & 0 \\ & & r_D^2 R_0 & r_D^2 R_0 & 0 & 0 \\ & & & & R_0 & 0 \\ \text{Symmetric} & & & & & 0 \\ & & & & & 0 \\ & & & & & 0 \end{bmatrix} \quad (16)$$

where

$$R_1 = \frac{-\pi}{M_d \omega^2} ; R_0 = \frac{-2\pi}{M_p \omega^2} \quad (17)$$

## 2.2 Receptances of a Multi-Stage Blade

In order to account for the twist, the blade is modelled as number of blade elements with different stagger angles, as shown in Fig. 2. Let there be 3 elements of a blade as shown in Fig. 3 and  $[\beta_1]$ ,  $[\beta_2]$  and  $[\beta_3]$  be the receptance matrices of elements 1, 2 and 3 respectively of 12 x 12 size corresponding to all six degrees of freedom at both the ends of each element; If the coupled receptance matrix for elements 1 and 2 be denoted as  $[\beta_{12}]$ , then

$$[\beta_{12}]^{-1} = [\beta_1]^{-1} + [\beta_2]^{-1} \quad (18)$$

Similarly, the coupled receptance matrix for elements 1, 2 and 3,  $[\beta_{123}]$ , may be obtained as

$$[\beta_{123}]^{-1} = [\beta_{12}]^{-1} + [\beta_3]^{-1} \quad (19)$$

The individual receptances of the blade can be obtained from Bishop & Johnson<sup>3</sup>. They are given in Appendix-A.

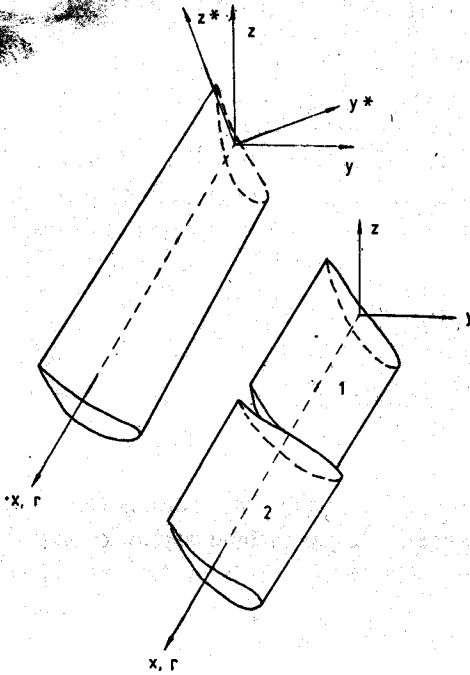


Figure 2. Pretwisted blade modelled as two staggered elements.

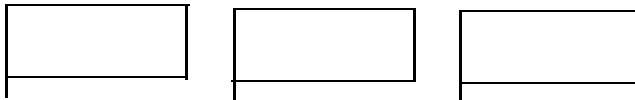


Figure 3. Coupling of blade elements.

### 2.3 Disk-Blade Interaction

Let  $\{q\}$  be a vector of the displacements and  $\{Q\}$  the internal loads in all 6 directions at a particular radius. Compatibility condition at the disk-rim/blade-root junction is

$$\{q\}_D = \{q\}_B \tag{20}$$

and equilibrium condition at the disk-rim/blade-root junction is

$$\{Q\}_D + \{Q\}_B = \{O\} \tag{21}$$

From the response/excitation relationships, we have

$$\{q\}_D = [\lambda] \{Q\}_D \tag{22}$$

and

$$\{q\}_B = [\beta] \{Q\}_B \tag{23}$$

Using Eqns. (20) to (23), a set of homogeneous linear equations may be obtained,

$$\{[\alpha] + [\beta]_B\} \{Q\}_D = 0 \quad (24)$$

in which variables are the forces at the junction between blade-root and disk-rim and the coefficients are the elements of the receptance matrices. In order that a set of homogeneous equations may have nontrivial solution the determinant of their coefficients must vanish. As the determinant in this case is composed of frequency dependent receptance expressions

$$|[\alpha] + [\beta]_B I - I \Delta(\omega) I| = 0 \quad (25)$$

As the disk receptances  $\alpha(n)$  are developed as a function of nodal diameters, the corresponding mode shapes can also be obtained.

A computer program is developed to determine the natural frequencies and mode shapes using the theory developed here. A gas-turbine assembly and third stage of compressor assembly were analyzed. The details for both the assemblies are given in Tables 1 and 2, to determine their natural frequencies and corresponding mode shapes. The results obtained are plotted in Figs. 4 and 5 along with the experimental results.

Table 1. Gas-turbine bladed-disk details

Weight of the assembly = 24.2 kg, No. of blades = 125, Coupling coordinates at the root of each blade = 6

#### Disk Details

Number of elements = 2

| Disk element (DE) | Inner radius* mm | Outer radius mm | Thickness mm | Density kg/cu m | Modulus of elasticity GN/sq m | Poisson's ratio |
|-------------------|------------------|-----------------|--------------|-----------------|-------------------------------|-----------------|
| 1                 | 115.50           | 230.00          | 7.00         | 7833.00         | 206.84                        | 0.287           |
| 2                 | 230.00           | 240.00          | 21.00        | 7833.00         | 206.84                        | 0.287           |

- The disk is fixed at the inner radius

#### Blade Details

Number of elements = 2

| Blade element (BE) | Area mm <sup>2</sup> | $I_{xx}$ mm <sup>4</sup> | $I_{yy}$ mm <sup>4</sup> | $J$ mm <sup>*</sup> | Length mm | Density kg/cu m | Modulus of elasticity GN/sq m | Stagger angle degree |
|--------------------|----------------------|--------------------------|--------------------------|---------------------|-----------|-----------------|-------------------------------|----------------------|
| 1                  | 61.08                | 147.91                   | 2123.90                  | 68.64               | 45.0      | 7833.00         | 206.84                        | 15                   |
| 2                  | 42.32                | 124.13                   | 1793.14                  | 50.28               | 45.0      | 7833.00         | 206.84                        | 25                   |

Table 2. Compressor assembly details

Third stage compressor bladed-disk details, Weight of the assembly = 14.6 kg  
 Number of blades = 3 1, Coupling coordinates at the root of each blade = 6

**Disk Details**

Number of elements = 3

| Disk element (DE) | Inner radius mm | Outer radius mm | Thickness mm | Density kg/cu m | Modulus of elasticity GN/sq m | Poisson's ratio |
|-------------------|-----------------|-----------------|--------------|-----------------|-------------------------------|-----------------|
| 1                 | 68.0            | 70.0            | 18.0         | 2699.00         | 68.84                         | 0.332           |
| 2                 | 70.0            | 174.0           | 7.0          | 2699.00         | 68.84                         | 0.332           |
| 3                 | 174.0           | 176.0           | 19.0         | 2699.00         | 68.84                         | 0.332           |

**Blade Details**

Number of elements = 2

| Blade element (BE) | Area mm <sup>2</sup> | I <sub>xx</sub> mm <sup>4</sup> | I <sub>yy</sub> mm <sup>4</sup> | J mm <sup>4</sup> | Length mm | Density kg/cu m | Modulus of Elasticity GN/sq m | Stagger angle degree |
|--------------------|----------------------|---------------------------------|---------------------------------|-------------------|-----------|-----------------|-------------------------------|----------------------|
| 1                  | 72.18                | 174.15                          | 3619.18                         | 81.86             | 69.0      | 2699.0          | 68.84                         | 18.0                 |
| 2                  | 54.76                | 155.44                          | 3142.14                         | 50.85             | 69.0      | 2699.0          | 68.84                         | 24.0                 |

**3. Experimental Work**

An MBIS, automatic servocontrolled, vibration exciter controlled by a 2600 series computer was used to excite the bladed-disk assembly, accurately at the desired frequency and level of excitation. The feed back MBIS accelerometer, mounted at the centre of the disk, controls the system with the desired abort limits of excitation. Another B & K accelerometer mounted on the disk, whose position could be changed, was used to monitor the response through a B & K 2511 vibration-meter. The signal was also monitored through a HP-3582A real time spectrum analyzer to detect the natural frequencies. Print out of the desired signal was obtained by HP-85 computer which was also connected to spectrum analyzer.

The gas-turbine and the compressor (third stage) assembly of an **orpheus** engine were mounted on the exciter through a fixture, designed for this purpose. In each case the natural frequencies, in the range of 10-2000 Hz were detected. The mode shape corresponding to each natural frequency was obtained by probing with the hand held accelerometer.

**4. Results and Discussion**

Details of both the gas-turbine and the compressor assemblies, used for the computation of natural frequencies and mode shapes are given in Tables 1 and 2 respectively.

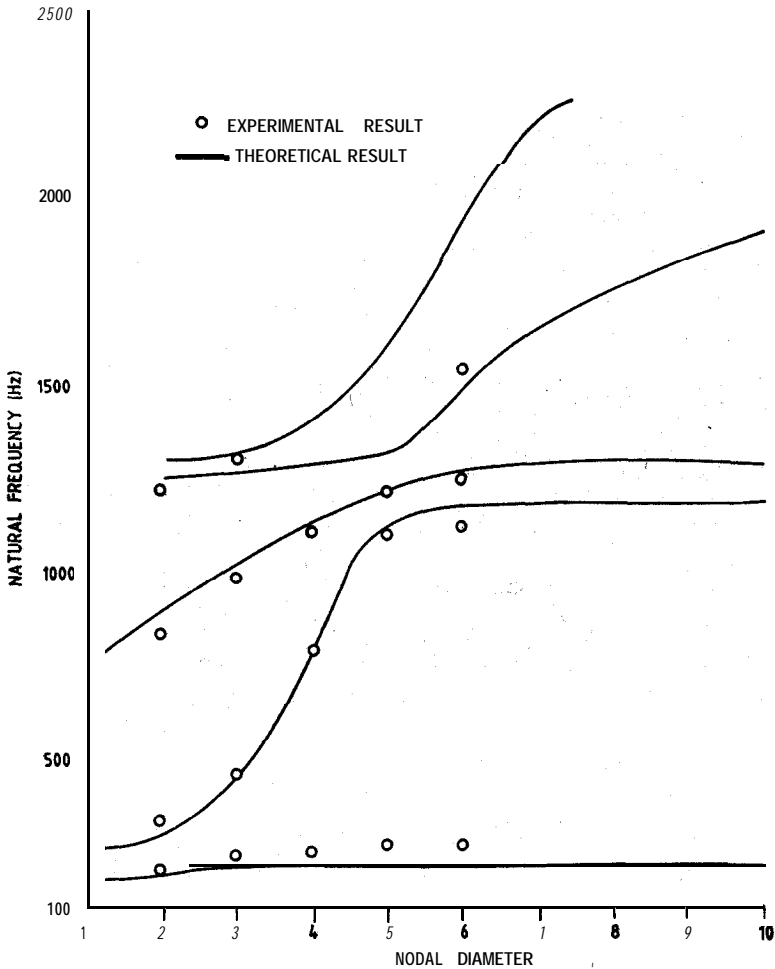


Figure 4. Natural frequency versus nodal diameter plots for gas turbine assembly.

The results obtained analytically as well as by experiments for various nodal circles are plotted as a function of nodal diameter in Figs. 4 and 5 respectively. The spectrum analyzer signals are shown in Figs. 6 to 9, for both the turbine and compressor assemblies.

It can be seen from Figs. 4 & 5 that there is an excellent agreement between the theoretical results and experimental values from one circle and above modes. In the case of compressor stage there is a large discrepancy in the results with more number of nodal diameters for zero circle modes. This discrepancy may be attributed to the material of the disc within the fixed domain as in Fig. 6 for turbine stage and due to large shaft portion within the disk in the case of compressor stage as in Fig. 8.

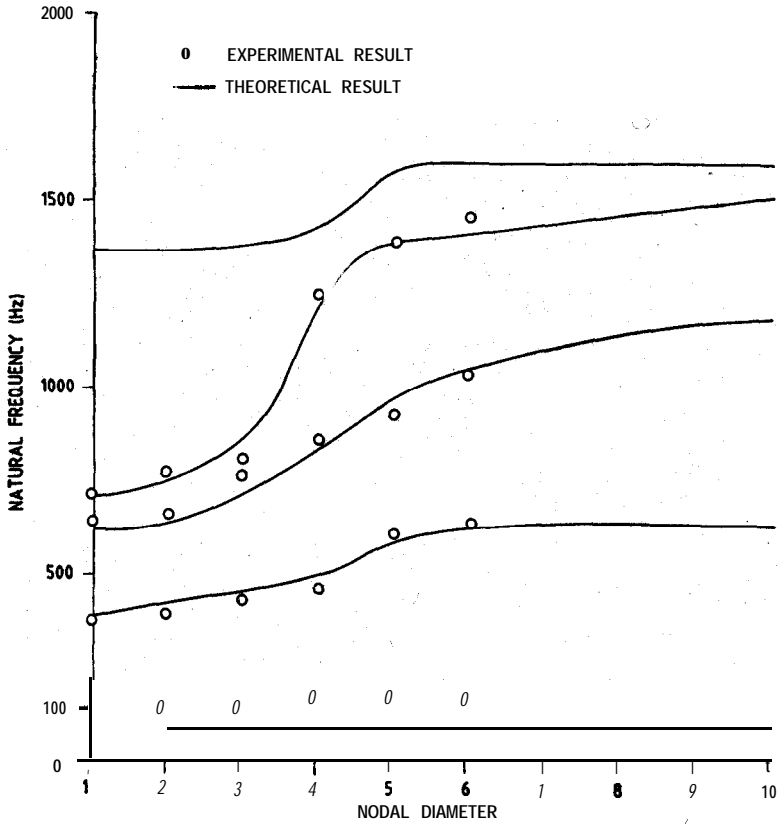
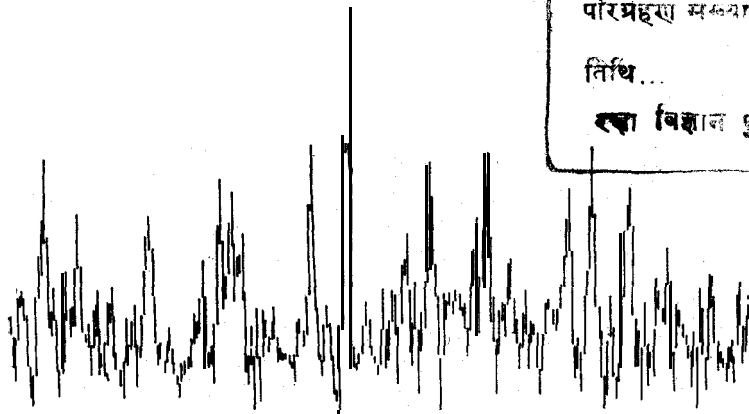


Figure 5. Natural frequency versus nodal diameter plots for third stage compressor assembly.

AMP : 64.50  $\mu$ v

293.6 Hz



डेसीडॉक  
परिग्रहण संख्या J-332  
तिथि...  
एवा विशाल पुस्तकालय

290 Hz

300 Hz

Figure 6. Signal analysis and mode shape of gas turbine assembly.

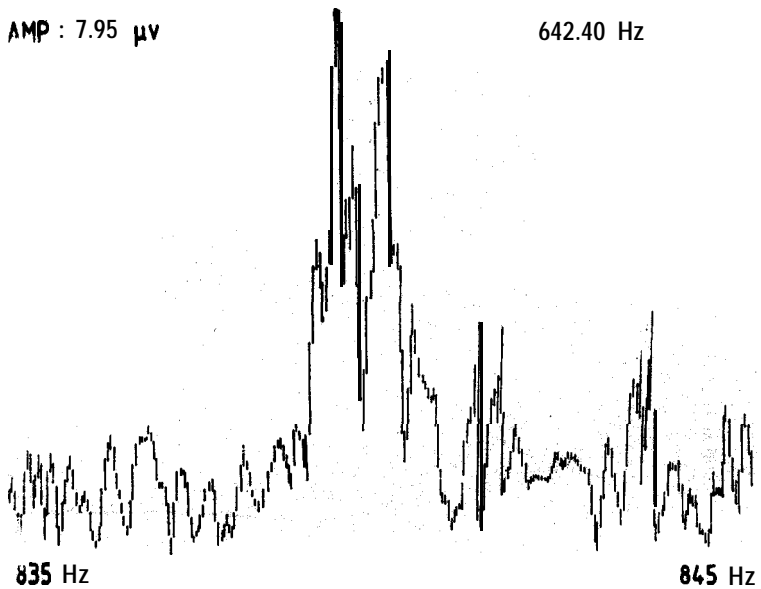


Figure 7. Signal analysis and mode shape of gas turbine assembly.

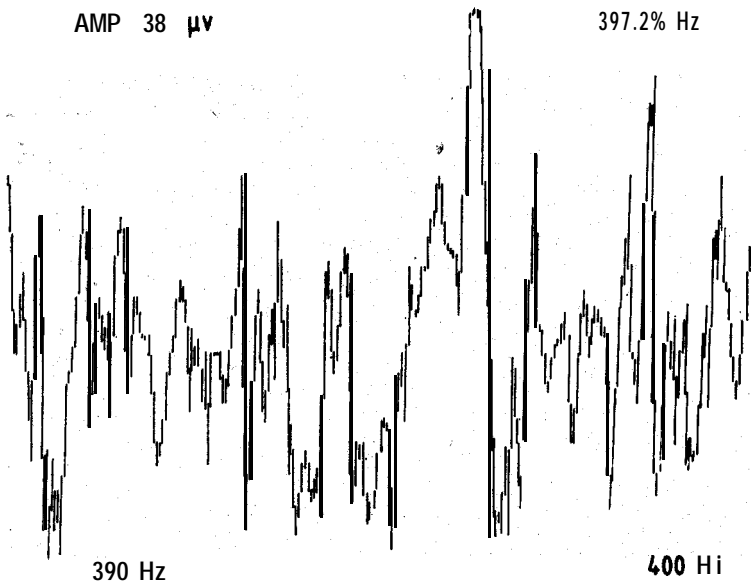


Figure 8. Signal analysis and mode shape of compressor assembly.

Otherwise it can be generally stated that the computer program developed here can be used to predict natural frequencies and mode shapes.

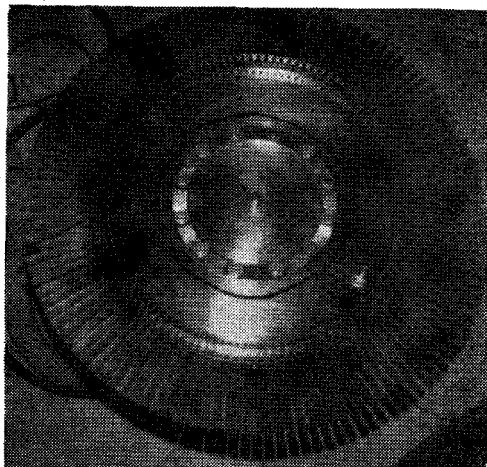


Figure 6

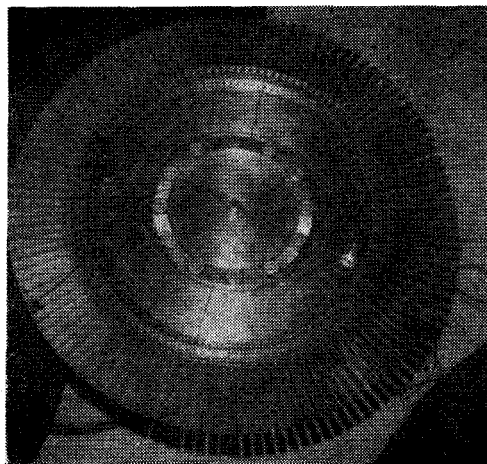


Figure 7

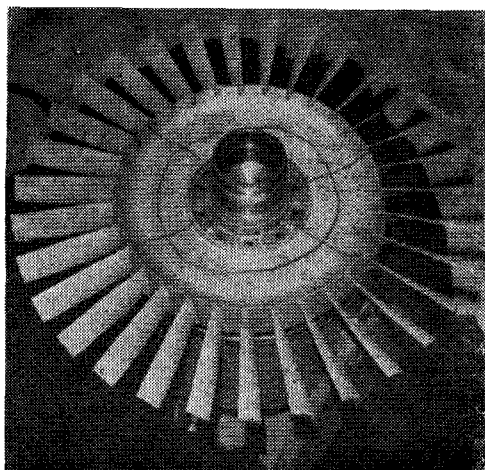


Figure 8

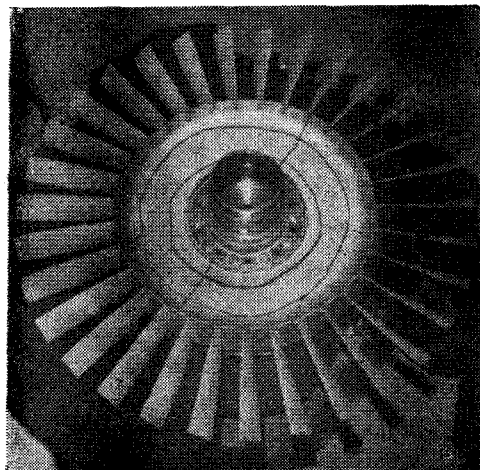


Figure 9

(Photographs of turbines and compressor assemblies corresponding to Figs. 6 to 9).

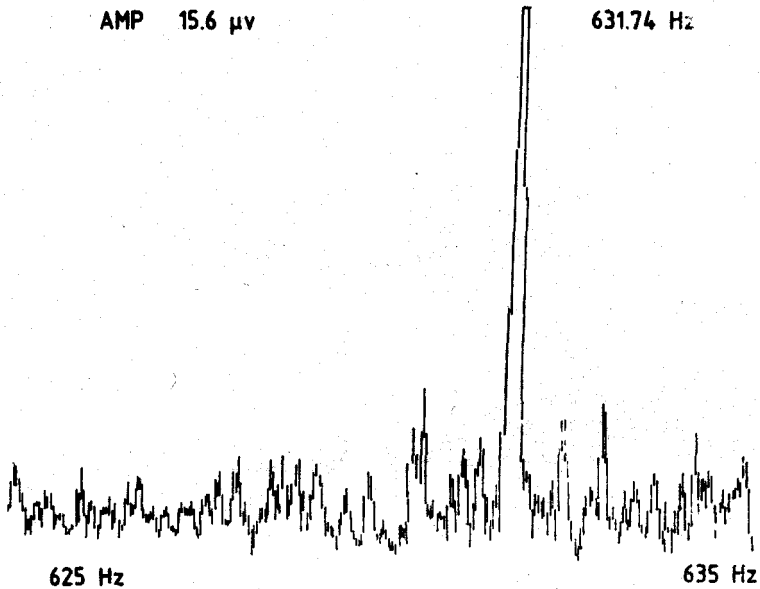


Figure 9. Signal analysis and mode shape of compressor assembly.

### Acknowledgement

The authors wish to acknowledge the support given by Aeronautical Research and Development Board, Ministry of Defence, by way of major project in undertaking this work.

### References

1. Armstrong, E. K., Ph.D. Thesis, University of Cambridge, 1955.
2. Armstrong, E. K., Christie, P. I. & Hauge, W. M., *Proc. Inst. Mech. Engg.*, 180 (1965), 110-123.
3. Bishop, R. E. D. & Johnson, D. C., 'The Mechanics of Vibration,' (Cambridge University Press), 1960.
4. Ewins, D. J., Ph. D. Thesis, University of Cambridge, 1966.
5. Ewins, D. J., *Journal of Sound and Vibrations*, 9 (1969), 65-79.
6. Ewins, D. J., *Journal of Mechanical Engineering Science*, 15 (1973), 165-186.
7. Cottney, D. J., **M.Sc.**, Thesis, Imperial College, 1971.
8. Cottney, D. J. & Ewins, D. J., *J. Engg. Industry, Trans. ASME* (1974), 1054.
9. McLeod, A. J. & Bishop, R. E. D., 'The Forced Vibration of Circular Flat Plates', *Mech. Engg. Sci.*, Monograph No. 1.
10. Ganesh, Ch. L., M. Tech. Thesis, I.I.T. Delhi, 1984.
11. Rao, J. S., et al., Report No. 285, Part-I, A.R. & D.B., Ministry of Defence, Govt. of India, 1984.

Receptances of an Element of a Blade

**(a) Receptances in Flexural Direction**

(i) Receptances at blade root

Direct receptance between force and displacement  $= \beta'_1 = -\frac{F_5}{EI \lambda^3 F_3}$

Cross receptance between force and slope  $= \beta'_2 = -\frac{F_1}{EI \lambda^2 F_3}$

Cross receptance between moment and displacement  $= \beta'_3 = \frac{-F_1}{EI \lambda^2 F_3}$

Direct receptance between moment and slope  $= \beta'_4 = \frac{F_6}{EI \lambda F_3}$

(ii) Receptances between blade root and tip

Direct receptance between force and displacement  $= \beta''_1 = \frac{F_8}{EI \lambda^3 F_3}$

Cross receptance between force and slope  $= \beta''_2 = \frac{-F_{10}}{EI \lambda^2 F_3}$

Cross receptance between moment and displacement  $= \beta''_3 = \frac{-F_{10}}{EI \lambda^2 F_3}$

Direct receptance between moment and slope  $= \beta''_4 = \frac{F_7}{EI \lambda F_3}$

(iii) Receptances at blade tip

Direct receptance between force and displacement  $= \beta'''_1 = \frac{-F_5}{EI \lambda^3 F_3}$

Cross receptance between force and slope  $= \beta'''_2 = \frac{F_1}{EI \lambda^2 F_3}$

Cross receptance between moment and displacement  $= \beta'''_3 = \frac{F_1}{EI \lambda^2 F_3}$

Direct receptance between moment and slope  $= \beta'''_4 = \frac{F_6}{EI \lambda F_3}$

**(b) Receptances in Edgewise Direction**

They are same as the flexural receptances but their signs in case of cross receptances should be changed for the proper directions, viz.,

$$- \beta'_2, - \beta'_3, - \beta''_2, - \beta''_3, - \beta'''_2 \text{ and } - \beta'''_3$$

where

$$F_1 = \sin \lambda L, \sinh \lambda L$$

$$F_3 = \cos \lambda L, \cosh \lambda L - 1$$

$$F_5 = \cos \lambda L, \sinh \lambda L - \sin \lambda L, \cosh \lambda L$$

$$F_6 = \cos \lambda L, \sinh \lambda L + \sin \lambda L, \cosh \lambda L$$

$$F_7 = \sin \lambda L + \sinh \lambda L$$

$$F_8 = \sin \lambda L - \sinh \lambda L$$

$$F_{10} = \cos \lambda L - \cosh \lambda L$$

**(c) Torsional Receptances**

$$\beta'_5 = -1/GJ\omega \sqrt{\frac{\rho}{G}} \cdot \tan(\omega \sqrt{\rho/G} L)$$

$$\beta''_5 = \beta'_5 / \cos(\omega \sqrt{\rho/G} L)$$

$$\beta'''_5 = \beta''_5$$

**(d) Receptances in Longitudinal Direction**

$$\beta'_6 = -1/\rho \cdot \omega^2 \cdot AL$$

$$\beta''_6 = \beta'_6$$

$$\beta'''_6 = \beta'_6$$